Symmetrized amplitudes of the helium-atom double photoionization

A. S. Kheifets*
Research School of Physical Sciences, The Australian National University, Canberra ACT 0200, Australia

Igor Bray†
Centre for Atomic, Molecular, and Surface Physics, School of Mathematical and Physical Sciences, Murdoch University, Perth 6150, Australia

(Received 20 August 2001; published 15 January 2002)

The symmetrized gerade and ungerade amplitudes of the helium atom double photoionization are extracted from the convergent close-coupling calculations at fixed excess energies of 9, 20, 40, and 60 eV above the double-ionization threshold, and varying energy-sharing ratios. The amplitudes are fitted with a simple Gaussian ansatz. Although some deviations from this ansatz are clearly visible, especially at small mutual angles, the fully resolved triple differential cross sections generated from the calculated and fitted amplitudes are very close. This observation lends support to the *practical parametrization* suggested by Cvejanović and Reddish [J. Phys. B 33, 4691 (2000)]. A more thorough testing of the ionization amplitudes can be achieved by performing a complete double-photoionization experiment and by making a comparison with other highly accurate and computationally intensive theories.

DOI: 10.1103/PhysRevA.65.022708 PACS number(s): 32.80.Fb, 31.25.−v

I. INTRODUCTION

Double photoionization (DPI or $\gamma,2e$ reaction) of the helium atom has been a challenging problem attracting a considerable interest from experimentalists and theorists alike. Until recently, the most detailed information on the DPI process can be extracted from the fully resolved triple differential cross section (TDCS) which determines the probability of the two photoelectrons being detected with the fully resolved momenta $\mathbf{k}_1$, and $\mathbf{k}_2$. The TDCS have been measured and calculated under a variety of conditions and a very substantial volume of experimental and theoretical data have been accumulated. Results prior to 2000 have been reviewed recently by Briggs and Schmidt [1]. Latest theoretical developments in the field include applications of the time-dependent close-coupling (TDCC) method [2] and the hyperspherical *R*-matrix method with semiclassical outgoing waves (HRM-SOW) [3]. A recently developed exterior complex scaling (ECS) method [4,5] also shows considerable promise in a related problem of the electron impact ionization of hydrogen. On the experimental side, the TDCS have been measured recently at 40 and 60 eV excess energies with improved resolution and statistics [6–8]. Generally, agreement between theory and experiment is satisfactory.

All nontrivial information on the DPI process is contained in a pair of the symmetrized amplitudes a_g and a_u that depend on the energies of the two photoelectrons E_1 and E_2 and their mutual angle θ_{12}. The indices g and u stand for gerade and ungerade, or symmetric and antisymmetric, with respect to the permutation of the two photoelectrons. It was demonstrated in an early work by Huetz *et al.* [10], extended by Malegat *et al.* [11,12], that only these two amplitudes are needed to construct the TDCS at an arbitrary geometry of the two-electron escape and any polarization composition of light.

The symmetrized amplitudes are the most fundamental characteristics of the DPI process. However, these amplitudes cannot be extracted from the TDCS measurements alone. For this purpose a complete DPI experiment is needed in which both moduli and phases of the ionization amplitudes are determined. A possibility of such an experiment utilizing the COLTRIMS technique has been demonstrated recently by Kraessig [9].

Long before a complete experiment became possible numerous attempts have been made to extract the DPI amplitudes from ''incomplete'' experiments in which only the TDCS have been measured. These attempts relied on a simple analytical representation of the DPI amplitudes fitted with a few adjustable parameters. Most of these studies have been focused on the symmetric amplitude. It fully defines the TDCS under the equal energy-sharing condition $E_1=E_2$ as the antisymmetric amplitude vanishes in this case. It is customary to apply a simple Gaussian parametrization to the squared symmetric amplitude (correlation factor). The Gaussian form follows from the Wannier-type quasiclassical theories [13,14] that are only valid at very small excess energies $E=E_1+E_2$ over the DPI threshold. There is no firm theoretical ground to apply this parametrization at large excess energies. Moreover, in a later theoretical study it was shown that the Wannier regime did not necessarily imply a Gaussian distribution over the correlation angle [15]. Nevertheless, by using the Gaussian ansatz as a simple practical tool a number of experimental TDCS have been described accurately at excess energies of 20 eV [12,16,17], 40 eV [6], and even 60 eV [18]. Fully numerical calculations [19] also supported the accuracy of the Gaussian parametrization at the energy range of 3–80 eV as far as the TDCS was concerned.

*Electronic address: A.Kheifets@anu.edu.au; URL: http://rsphysse.anu.edu.au/~ask107

†Electronic address: I.Bray@murdoch.edu.au; URL: http://yin.ph.flinders.edu.au/igor.html

More recently, a similar ''practical'' parametrization has been applied to the antisymmetric amplitude that is essential to describe the TDCS at an unequal energy sharing between the photoelectrons ($R=E_1/E_2\neq 1$) [20]. In the simplest three-parameter (3P) model both the symmetric and antisymmetric amplitudes were described by the Gaussians of the same width. In a more sophisticated four-parameter (4P) model the symmetric and antisymmetric amplitudes were allowed to have different widths.

The 3P model was shown to describe adequately the experimental TDCS at the excess energy of 40 [6] and 60 eV [18]. In fact, the simulated TDCS were closer to the experimental data than *ab initio* calculations using the product of three Coulomb waves (3C method) [21] and the convergent close-coupling (CCC) method [22]. Both the 3P and 4P models were applied by Bolognesi *et al.* [7] at the excess energy of 40 eV. The 4P model was found to fit the experimental data better than the 3P model. The Gaussian width of the antisymmetric amplitude was substantially smaller than that of the symmetric amplitude. Again, as in the case of Cvejanović and Reddish [20], the simulated TDCS were closer to the measured ones than the *ab initio* calculations using the 3C and CCC models.

In addition to the somewhat empirical Gaussian parametrization, an exact recipe was suggested by Malegat, Selles, and Huetz [11] to parametrize both the symmetric and antisymmetric amplitudes by expanding them over the cosine power series of the mutual angle θ_{12}. The coefficients of this expansion are to be found by fitting the experimental TDCS. Malegat *et al.* [12] tested this recipe on the measured equal energy-sharing TDCS at the excess energy of 4 and 18.6 eV [23] while truncating the expansion with respect to the one-electron angular momentum to $l_{\max}=4$. The resulting symmetric amplitudes were practically indistinguishable from a Gaussian. A hybrid parametrization was employed by Soejima *et al.* [24] who analyzed both equal and unequal energy-sharing TDCS at the excess energy of 9 eV. The symmetric amplitude was fitted with a Gaussian on a constant background. The much smaller antisymmetric amplitude was fitted with a full cosine expansion as suggested by Malegat, Selles, and Lablanquie [11]. Although a good fit to the experimental TDCS was obtained, a large number of fitting parameters employed by Soejima *et al.* [24] made their fitting process ambiguous, as was demonstrated subsequently by Cvejanović and Reddish [20].

In this paper, we extract the symmetrized amplitudes from the CCC calculation to allow for subsequent most detailed comparison with the complete experiment and other calculations. We demonstrate that the CCC method is fully compliant with the general cosine power-series formalism of Malegat, Selles, and Huetz [11]. However, a large number of terms in this expansion makes it impractical to tabulate the expansion coefficients and use them as a reference base. Instead, we use the Gaussian ansatz to quantify our data by fitting the amplitudes with the 4P formula of Cvejanović and Reddish [20]. Although some deviations from the Gaussian ansatz are clearly visible, especially at small mutual angles, the TDCS generated from the calculated and fitted amplitudes are very close. This observation lends support to the ''practical'' parametrization of Cvejanović and Reddish [20] as a useful and convenient tool to analyze experimental TDCS. However, a more physically meaningful analysis can go beyond the TDCS and be focused on the ionization amplitudes themselves.

The rest of the paper is organized as follows. In Sec. II, we give a brief outline of the CCC theory and arrive at the cosine expansion of the symmetrized amplitudes equivalent to the one proposed by Malegat, Selles, and Huetz [11]. Computation details are given in Sec. III. Results are summarized and discussed in Sec. IV.

II. FORMALISM

We write the TDCS as

$$\frac{d^3\sigma_M}{d\Omega_1\, d\Omega_2\, dE_1}\equiv\sigma_M=|T_M|^2, \tag{2.1}$$

where M is the angular momentum projection of the photon. We choose the frame in which the photon is propagating along the x axis and the major polarization axis of light is directed along the z axis. The light is characterized by the Stokes parameters S_1, S_3 and the TDCS is given by the formula [25]

$$\begin{aligned}\sigma(S_1,S_3)&=\frac{1}{2}(\sigma_z+\sigma_y)+\frac{S_1}{2}(\sigma_z-\sigma_y)+\frac{S_3}{2}(\sigma_+-\sigma_-)\\&\equiv\Delta_0+S_1\Delta_L+S_3\Delta_C.\end{aligned} \tag{2.2}$$

Here the polarization independent (PI), linear dichroism (LD)$\propto S_1$, and circular dichroism (CD)$\propto S_3$ terms have been isolated. In our notation the two linear polarized components σ_z, σ_y are equal to σ_0, σ_1, respectively. The two circular polarized components $\sigma_\pm$ can be expressed as

$$\sigma_\pm=\tfrac{1}{2}|T_0\pm iT_1|^2.$$

Therefore, the TDCS can be presented as

$$\sigma(S_1,S_3)=\frac{1+S_1}{2}|T_0|^2+\frac{1-S_1}{2}|T_1|^2-S_3\,\mathrm{Im}(T_0^*T_1). \tag{2.3}$$

As in our previous work [22,26], we introduce the partial-wave expansion

$$\sigma_M=\frac{1}{3}C\left|\sum_{l_1l_2}B_{1M}^{l_1l_2}(\hat{\mathbf{k}}_1,\hat{\mathbf{k}}_2)D_{l_1l_2}(E_1,E_2)\right|^2, \tag{2.4}$$

where $C=8\pi^2\omega/c$ is the photoionization constant expressed through the photon energy ω and the speed of light in atomic units $c\simeq 137$. The bipolar spherical harmonics [27] for the angular momentum of the photon $L=1$ are

$$B_{1M}^{l_1l_2}(\hat{\mathbf{k}}_1,\hat{\mathbf{k}}_2)=\sum_{m_1m_2}C^{1M}_{l_1m_1l_2m_2}Y_{l_1m_1}(\hat{\mathbf{k}}_1)Y_{l_2m_2}(\hat{\mathbf{k}}_2). \tag{2.5}$$

They depend on the unit vectors $\hat{\mathbf{k}}_i = \mathbf{k}_i / k_i$, $i = 1,2$ and satisfy the relation

$$B_{1M}^{l+1l}(\hat{\mathbf{k}}_1, \hat{\mathbf{k}}_2) = B_{1M}^{ll+1}(\hat{\mathbf{k}}_2, \hat{\mathbf{k}}_1), \tag{2.6}$$

which we will use later. The reduced matrix elements $D_{l_1 l_2}(E_1, E_2)$ are to be evaluated within some numerical approximation, but must satisfy the symmetry relation

$$D_{l_1 l_2}(E_1, E_2) = D_{l_2 l_1}(E_2, E_1) \tag{2.7}$$

owing to indistinguishability of electrons.

The angular momentum summation in Eq. (2.4) can be reduced to the sum over a single variable

$$\sigma_M = \frac{1}{3} C \left| \sum_{l=0}^{\infty} B_{1M}^{ll+1}(\hat{\mathbf{k}}_1, \hat{\mathbf{k}}_2) D_{ll+1}(E_1, E_2) + B_{1M}^{l+1l}(\hat{\mathbf{k}}_1, \hat{\mathbf{k}}_2) D_{l+1l}(E_1, E_2) \right|^2 . \tag{2.8}$$

After we introduce symmetric and antisymmetric combinations of the matrix elements

$$D_{l_1 l_2}^{\pm}(E_1, E_2) = \tfrac{1}{2} \{ D_{l_1 l_2}(E_1, E_2) \pm D_{l_1 l_2}(E_2, E_1) \}, \tag{2.9}$$

we have

$$\sigma_M = \frac{1}{3} C \left| \sum_{l=0}^{\infty} D_{ll+1}^{+}(E_1, E_2) [B_{1M}^{ll+1}(\hat{\mathbf{k}}_1, \hat{\mathbf{k}}_2) + B_{1M}^{ll+1}(\hat{\mathbf{k}}_2, \hat{\mathbf{k}}_1)] + D_{ll+1}^{-}(E_1, E_2) [B_{1M}^{ll+1}(\hat{\mathbf{k}}_1, \hat{\mathbf{k}}_2) - B_{1M}^{ll+1}(\hat{\mathbf{k}}_2, \hat{\mathbf{k}}_1)] \right|^2 . \tag{2.10}$$

For simplicity, we initially consider the DPI by light fully polarized along the z direction ($S_1 = 1$, $S_3 = 0$). In this case $M = 0$ and we can use expressions for the bipolar spherical harmonics derived by Kono and Hattori [28]

$$B_{10}^{ll+1}(\hat{\mathbf{k}}_1, \hat{\mathbf{k}}_2) = \frac{(-1)^l}{4\pi} \left(\frac{3}{l+1} \right)^{1/2} \{ \cos\theta_2 P'_{l+1}(\cos\theta_{12}) - \cos\theta_1 P'_l(\cos\theta_{12}) \}, \tag{2.11}$$

where $\cos\theta_{12} = \hat{\mathbf{k}}_1 \cdot \hat{\mathbf{k}}_2$. This immediately takes us to the final expression

$$\sigma_0 = C | (\cos\theta_1 + \cos\theta_2) a_g(E_1, E_2) + (\cos\theta_1 - \cos\theta_2) a_u(E_1, E_2) |^2, \tag{2.12}$$

where the symmetric and antisymmetric DPI amplitudes are

$$a_{u}^{g}(E_1, E_2) = \frac{1}{4\pi} \sum_{l=0}^{\infty} \frac{(-1)^l}{\sqrt{l+1}} [P'_{l+1}(\cos\theta_{12}) \mp P'_l(\cos\theta_{12})] D_{ll+1}^{\pm}(E_1, E_2). \tag{2.13}$$

By using the properties of the Legendre polynomials [29] the angular factors in Eq. (2.12) can be transformed to the angular functions introduced by Malegat, Selles, and Huetz [11]

$$F_{l+1}^{g}(\cos\theta_{12}) = (l+1) P_l(\cos\theta_{12}) + (\cos\theta_{12} \mp 1) P'_l(\cos\theta_{12}). \tag{2.14}$$

For light polarized along the y direction, we should substitute the cosine functions in Eq. (2.12) with the sine ones. More general expressions can be derived for arbitrary polarization if the two photoelectrons are detected in the polarization plane of light (the so-called coplanar geometry):

$$\begin{aligned} \Delta_0 &= |a_g|^2 [1 + \cos\theta_{12}] + |a_u|^2 [1 - \cos\theta_{12}], \\ \Delta_L &= |a_g|^2 [\cos^2\theta_2 - \sin^2\theta_1 + \cos(\theta_1 + \theta_2)] \\ &\quad + |a_u|^2 [\cos^2\theta_2 - \sin^2\theta_1 - \cos(\theta_1 + \theta_2)] \\ &\quad - 2\,\mathrm{Re}(a_g a_u^*) [\sin^2\theta_2 - \sin^2\theta_1], \\ \Delta_C &= 2\,\mathrm{Im}(a_g a_u^*) \sin\theta_{12}. \end{aligned} \tag{2.15}$$

III. COMPUTATION DETAILS

A. CCC method

We use the CCC method to estimate the matrix elements $D_{l_1 l_2}(E_1, E_2)$ and then to plug them into the cosine power-series expansion (2.13) to determine the amplitudes a_g and a_u. In the CCC method the two photoelectrons are treated on a different footing. The higher energy electron (labeled here as 1) is represented by true Coulomb waves in each partial wave channel whereas the lower-energy electron (labeled as 2) is described by the matching positive-energy bound pseudostates. The method expands the final-state wave function using $N = \Sigma_{l=0,l_{\max}} N_l$ pseudostates [22]. The resultant matrix elements $d_{l_1 l_2}^{(N)}(E_1, E_2)$ are not symmetric on the interchange of electron labels as required. In fact, with increasing N, they appear to converge to a step function with $d_{l_1 l_2}^{(N)}(E_1, E_2) \to 0$ for $E_2 > E_1$, where E_2 is the energy of a pseudostate. This behavior is identical to that found in the model e-H scattering problem [30], and is related to the unequal treatment of the two outgoing electrons within a unitary formalism. Stelbovics [31] showed that the correctly symmetrized CCC amplitudes could be obtained generally only if the step function was satisfied. In the present case the required amplitude is constructed as

$$D_{l_1 l_2}^{(N)}(E_1, E_2) = d_{l_1 l_2}^{(N)}(E_1, E_2) + d_{l_2 l_1}^{(N)}(E_2, E_1). \tag{3.1}$$

Note that for $E_1 \neq E_2$ the energy separation of the pseudostates ensures that one of the two terms above is dominant. For $E_1 = E_2$, and sufficiently large $l_{\max}$ and N_l we find that $d_{l_1 l_2}^{(N)} \approx d_{l_2 l_1}^{(N)}$, and hence (3.1) leads to a doubling of the raw CCC-calculated amplitude. This issue has been studied in great detail in the case of e-H ionization by Bray [32]. As a consequence of the work by Stelbovics [31] the close-

coupling expansion behaves similar to a Fourier expansion of a step function with convergence at the step to half the step height. This explains the oscillations observed when the step height is nonzero for $E_1 \neq E_2$, and yet apparent convergence at $E_1 = E_2$ [30].

With this understanding it is clear that we require infinite N to obtain convergence for $D^{(N)}_{l_1 l_2}(E_1, E_2)$ whenever $E_1 \neq E_2$. As this is not practical we rely on a procedure that averages over the oscillations. Since we know the result at $E_1 = E_2$ *ab initio*, the oscillations for $E_2 \ll E_1$ are not particularly large [30], the integral over the energy (closure relation), and that the underlying energy variation is likely to be smooth, the error associated with any sensible energy-averaging procedure is likely to be small. Note that we have no control over the angular distributions arising from $D^{(N)}$, which we require to show convergence with increasing N.

Thus, in CCC calculations we take $E_1 \geqslant E_2$ and hence $R = E_1/E_2 \geqslant 1$. The symmetrized amplitudes for reciprocal energy sharings $R < 1$ are found by the permutation rule:

$$a_g(E_1, E_2) = a_g(E_2, E_1), \quad a_u(E_1, E_2) = -a_u(E_2, E_1), \tag{3.2}$$

which follows from the symmetry relation (2.7) and the definition (2.9).

B. Gaussian parametrization

The complex amplitudes a_g, a_u can be written as $a_g = A_g \exp(i\delta_g)$, $a_u = A_u \exp(i\delta_u)$, where A_g, A_u, δ_g, and δ_u are real. The cross product $a_g a_u^*$ that enters the LD and CD terms in Eq. (2.15) can be presented as $A_g A_u \exp(i\phi)$, where the phase difference $\phi = \delta_g - \delta_u$.

We introduce the Gaussian ansatz for the real amplitudes A_g, A_u:

$$A_g = b_g \exp\left[-2 \ln 2 \frac{(\pi - \theta_{12})^2}{\Gamma_g^2}\right],$$

$$A_u = b_u \exp\left[-2 \ln 2 \frac{(\pi - \theta_{12})^2}{\Gamma_u^2}\right]. \tag{3.3}$$

Under the assumption of a constant phase shift ϕ for all mutual angles θ_{12} (3.3) is equivalent to the 4P parametrization of Cvejanović and Reddish [20] with the four parameters being the two Gaussian widths Γ_g, Γ_u, the magnitude ratio $\eta = b_u/b_g$, and the phase shift ϕ. These four parameters are sufficient to construct a relative TDCS. The five parameters (two magnitudes, two widths, and phase shift) are needed to obtain a normalized TDCS. All of these parameters depend on the total excess energy E and energy-sharing ratio R. The special case of equal energy sharing $R = 1$ was extensively studied in our earlier paper [19]. In this case $\eta = 0$. By virtue of the Coulomb zone $\Gamma_u \to \Gamma_g$.

IV. RESULTS AND DISCUSSION

We performed a series of CCC calculations at the excess energies of $E = 9$, 20, 40, and 60 eV above the double-ionization threshold. The choice of these energies was dictated by the availability of the experimental TDCS (see Table I). For each total excess energy E, we first performed the equal energy-sharing calculation $E_1 = E_2 = E/2$. These calculations yielded similar results to those used in our earlier study [19]. Each calculation had a total of $N = 105$ states with the maximum orbital angular momentum $l_{\max} = 5$ and the number of states for each l being $N_l = 20 - l$. The Laguerre exponential fall-off parameters $\lambda_l \approx 1.5$ were varied a little so that one of the states had the energy E_2. With these choices, for a given E, there were always the same number of positive-energy states for each l. This resulted in a similar energy distribution of states from 0 to $E/2$ for each l. Accordingly, unequal energy-sharing calculations $R > 1$ were able to be performed for input parameters almost identical to those used for $R = 1$. The number of different R calculated for a given E depended on the number of states with energy below $E/2$. Specifically, for $E = 9$, 20, 40, and 60 eV the R values calculated were (17, 5, 2.5, 1), (17, 8, 4, 2.2, 1), (79, 25, 12, 7, 4, 2.2, 1), and (39, 19, 11, 6.5, 3.8, 2.2, 1), respectively. Will present here just a small representative selection of the results. The complete set may be obtained electronically upon request.

TABLE I. Helium TDCS measurements at excess energies of 9, 20, 40, and 60 eV.

Excess energy E (eV)	Energy-sharing ratio $R = E_1/E_2$	Reference
9	1, 2, 8	[24]
20	1	[33]
	1	[16]
	0.11, 1, 9	[34]
	0.025, 0.053, 0.176, 0.25, 1, 1.86, 4, 5.67, 20, 40	[35]
	0.025, 0.081, 0.14, 0.38, 0.6	[36]
	1	[17]
40	1, 3, 7	[6]
	0.14, 7	[7]
60	1, 5, 11	[8]

A. Gaussian parameters

We applied the Gaussian ansatz (3.3) to the CCC calculated amplitudes A_g, A_u using a nonlinear least-χ^2 algorithm of Levenberg and Marquadt. Convergence of the fitting procedure was very fast. The error bars of the resulting parameters were typically less than 1%. The phase difference $\phi = \delta_g - \delta_u$ was extracted from the calculated amplitudes near the center of the Gaussians $\theta_{12} \simeq \pi$ where it was found to be approximately constant.

In Fig. 1, we show a typical example of the CCC calculated amplitudes A_g, A_u and their phases δ_g, δ_u as functions of the mutual angle θ_{12}. An excess energy of 40 eV is chosen and results for varying energy-sharing ratios R are presented. We see that the central portion of both the A_g and A_u amplitudes around $\theta_{12} = 180°$ has the characteristic Gaussian shape. The central area of the mutual angles $90° < \theta_{12}$

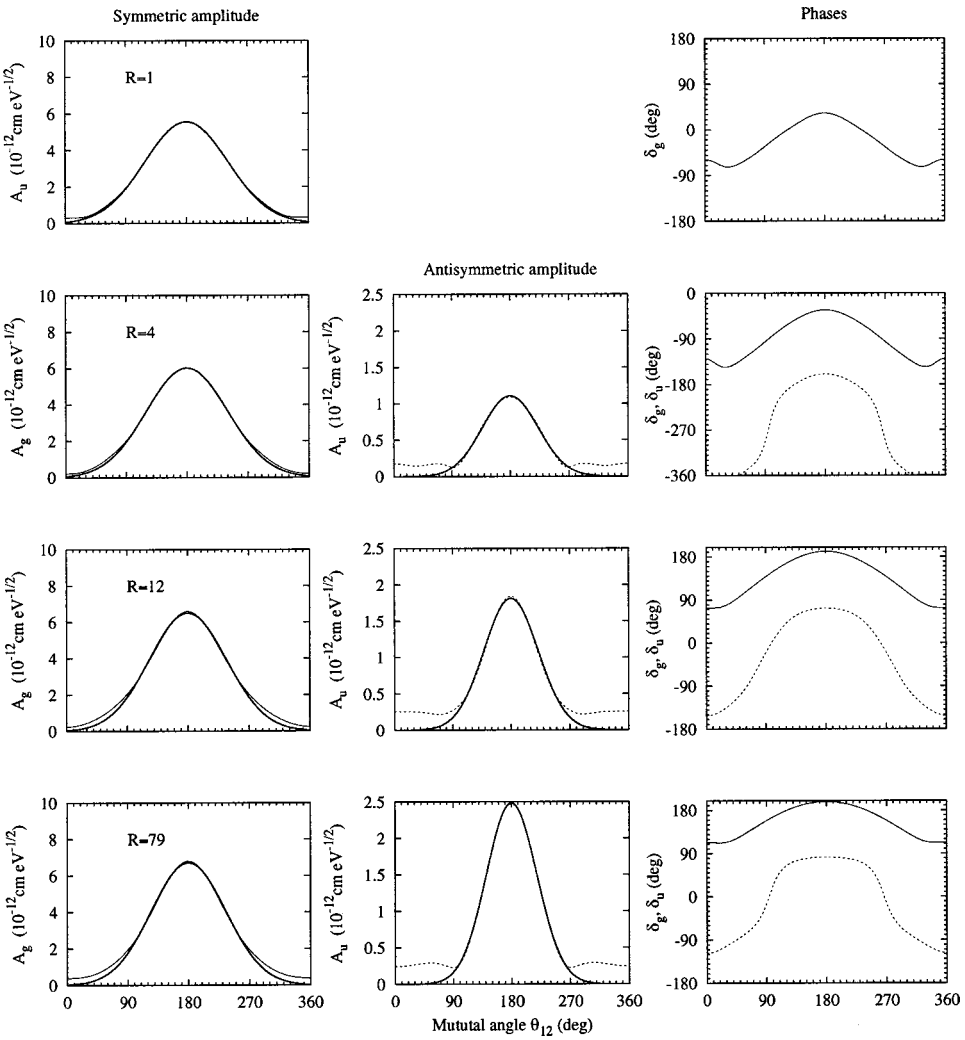

FIG. 1. Symmetrized amplitudes A_u (left panel), A_g (central panel), and their phases δ_u, δ_g (right panel) at $E=E_1+E_2=40$ eV and various energy-sharing ratios $R=E_1/E_2$. The symmetric and antisymmetric amplitudes and phases are shown by the solid and dashed lines, respectively. The thick solid line on the amplitude plots is the Gaussian parametrization (3.3).

$<270°$ was fitted with the Gaussian ansatz (3.3) and results of this fit are also presented in Fig. 1. The phase difference $\phi=\delta_g-\delta_u$ can be approximated by a constant in the central area.

At small mutual angles $\theta_{12}<90°$ or, equivalently, $\theta_{12}>270°$, the amplitudes noticeably deviate from the Gaussian shape, especially the antisymmetric amplitude A_u that shows substantial "wings." In the area of the wings the phase δ_g shows some rapid variation and the phase shift ϕ no longer remains constant. It is clear that the present calculations do not support the Gaussian ansatz across the entire angular range for the antisymmetric amplitude A_u, though we shall see this has little effect on the TDCS.

The central and peripheral parts of the amplitudes A_g, A_u reflect quite different escape regimes. At the mutual angles close to 180° the two photoelectrons propagate back-to-back. This is the well-known configuration of the Wannier escape that gives rise to the near-threshold law of the double ionization. However, this escape configuration only exists in the Coulomb zone and is strongly suppressed in the asymptotic region of large distances due to the dipole selection rules. The fact that the amplitudes A_g, A_u are very well represented by the Gaussian shape near $\theta_{12}=180°$ means that the Wannier regime dominates the back-to-back escape even at very high excess energies.

The peripheral region of small θ_{12} reflects upon a parallel escape of the two photoelectrons. This escape is strictly forbidden for the equal energy sharing but becomes possible as $E_1\neq E_2$. The parallel escape configuration is particularly sensitive to the symmetry of the two-electron wave function that provides a stringent test of the CCC formalism since the two photoelectrons are treated differently.

The parameters extracted from the Gaussian fit are summarized in Fig. 2 for all the excess energies and energy-sharing ratios studied in this paper. To extract values of the parameters at arbitrary energy-sharing ratios a polynomial interpolation is made to the data that is shown in the figure by solid lines. This interpolation is made under assumption that $\Gamma_u=\Gamma_g$ and $A_u=0$ as $R\to 1$. This assumption seems quite natural because in this case both the symmetrized amplitudes are made from the very similar nonsymmetrized amplitudes. There is no plausible hypothesis regarding the phase difference as $R\to 1$.

Despite some minor numerical instability the Gaussian parameters follow well-reproduced trends. The antisymmetric Gaussian width Γ_u is much smaller than its symmetric

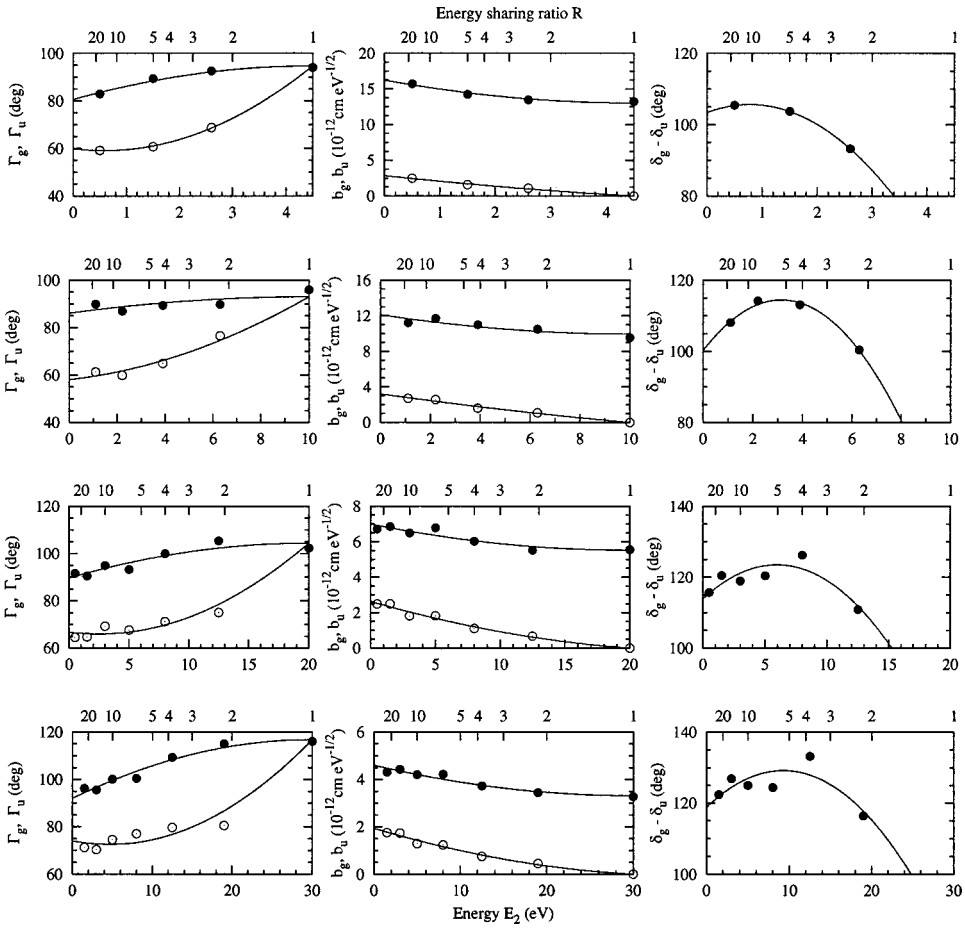

FIG. 2. Results of the Gaussian parametrization (3.3) at the excess energies of $E=9$, 20, 40, and 60 eV (from top to bottom). The width parameters Γ_u, Γ_g (left panel), the amplitude parameters b_g, b_u (central panel), and the phase difference $\phi=\delta_g-\delta_u$ (right panel) are plotted as functions of the slow electron energy $E_2 \leqslant E/2$ (bottom horizontals scale) or, equivalently, the energy-sharing ratio $R=E_1/E_2$ (top horizontal scale). Gerade and ungerade parameters are shown with filled and open circles, respectively. Calculations are performed at selected values of $R \geqslant 1$. The solid lines are a polynomial fit to the data.

counterpart Γ_g, contrary to the implicit assumption of the 3P model of Cvejanović and Reddish [20]. At the lower total energies of 9 and 20 eV the calculated width parameters show a clear tendency of Γ_u approaching Γ_g as $R \to 1$, as was assumed. More energy-sharing points between $R=1$ and 2 are needed to prove this tendency at the higher excess energies of 40 and especially 60 eV, though there is little practical value in determining the width of a Gaussian whose magnitude vanishes. Both the symmetric and antisymmetric magnitudes grow with R towards more asymmetric energy sharings. The phase difference ϕ demonstrates a nonmonotonic dependence on the energy-sharing ratio and peaks at $R \simeq 5$. The parameters given in this figure may be used to readily obtain theoretical TDCS for comparison with available experiment summarized in Table I.

B. TDCS

To demonstrate utility of the Gaussian parametrization (3.3) we construct the TDCS from the calculated and fitted amplitudes. We choose the particular case of 40 eV excess energy and the energy-sharing ratio of 7 ($E_1=35$ eV, $E_2=5$ eV). These kinematics were thoroughly analyzed by Cvejanović *et al.* [6], Cvejanović and Reddish [20]. In addition, Bolognesi *et al.* [7] studied both the case of $R=7$ and the complementary kinematics of $R=1/7$. Both authors applied the 3P parametrization and Bolognesi *et al.* [7] used the 4P parametrization as well.

In Fig. 3, we show the TDCS as a function of the variable escape angle of the fast electron ($E_1=35$ eV) at several selected escape angles of the slow photoelectron ($E_2=5$ eV). The three sets of theoretical amplitudes are shown: the CCC calculation and the two Gaussian fits with the parameters extracted from the present calculation and the experiment of Cvejanović *et al.* [6]. The values of these parameters are given in Table II. The margins on the presently calculated Gaussian parameters reflect numerical stability of our data. These margins are estimated as deviation of the ''raw'' calculated parameters from a smooth interpolated curve in Fig. 2.

First, we observe that the TDCS generated from the CCC calculated and CCC-fitted amplitudes are hardly discernible. This is despite the fact that the CCC amplitudes, especially the antisymmetric one, noticeably deviate from the Gaussian ansatz, as can be seen from Fig. 1. However, this deviation takes place only in the peripheral region where both the A_g and A_u are relatively small. As the TDCS is quadratic with respect to the amplitudes, the deviation from the Gaussian ansatz can hardly be noticed.

Next, we compare the calculated and experimental TDCS. Agreement is generally good, as was previously noted by Cvejanović *et al.* [6]. However, there is some deviation from the experiment for near parallel escape. In these cases the very simple 3P parametrization of Cvejanović and Reddish [20] reproduces the experiment a little better than the CCC

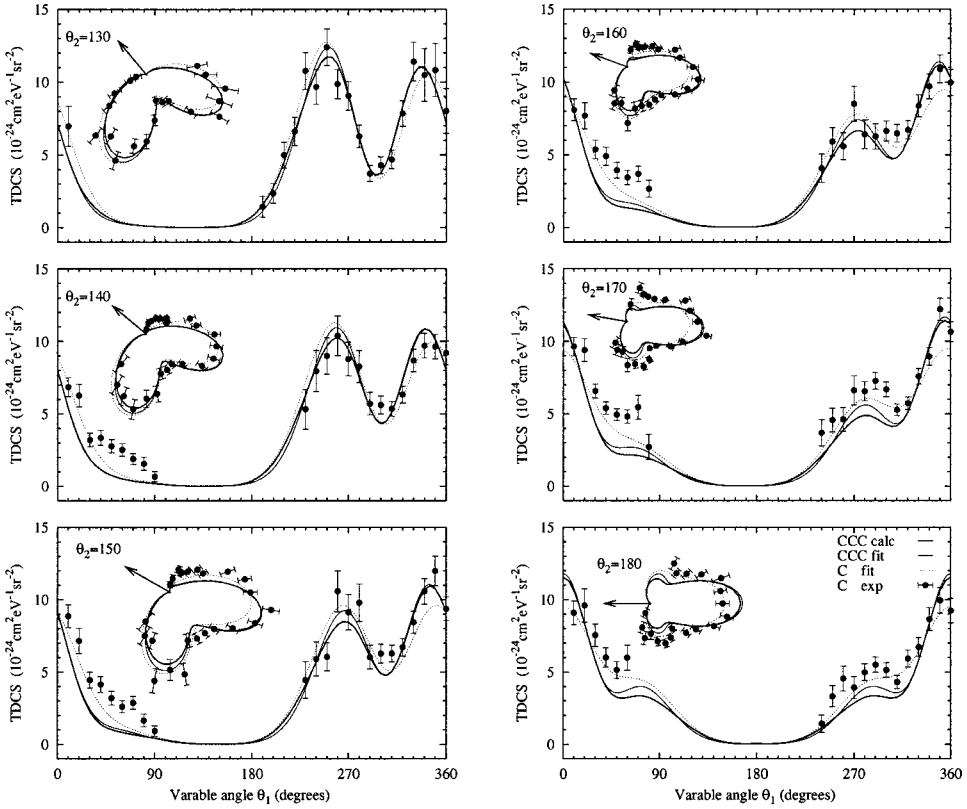

FIG. 3. DPI TDCS of helium at $E=40$ eV and energy-sharing ratio $R=E_1/E_2=7$. The arrow on the polar plots indicates the direction of the slower ($E_2=5$ eV) electron. The thick solid line is the CCC calculation (velocity form, other gauges near identical), the thin solid line is the 4P model with the Gaussian parameters extracted from the CCC calculation, the dashed line is the 3P model with the parameters from Cvejanović and Reddish [20]. Experimental data shown with error bars are from Cvejanović *et al.* [6].

calculation. This, we have to argue, is fortuitous as both the physical arguments and our numerical simulations suggest that the 3P assumption that the ''Gaussian width'' for both amplitudes is the same, is not correct. We also note that at 60 eV excess energy the CCC calculation was found in agreement with the measurement of Dawson *et al.* [8] for all the escape geometries, including parallel escape.

V. CONCLUSION

In the present study, we performed a series of CCC calculations of the symmetrized amplitudes of the helium atom DPI at several fixed excess energies and varying energy-sharing ratios. Owing to extensive discussion in the literature of various Gaussian parametrizations, we have provided Gaussian fits obtained directly from the theory. Indeed, in all cases studied the amplitudes are close in shape to Gaussians, though of substantially different widths for the symmetric and antisymmetric amplitudes. The phase difference between the amplitudes is approximately constant at mutual angles close to 180°. This suggests the 4P Gaussian parametrization of the amplitudes as proposed by Cvejanović and Reddish [20], ahead of the 3P model that assumes the same Gaussian width for both amplitudes. The physical justification of the 4P parametrization is in the fact that the back-to-back emission of the photoelectron pair follows the Wannier regime even at very high excess energies far above the double ionization threshold.

Utility of the 4P Gaussian parametrization is illustrated in the case of 40 eV excess energy with $E_1=35$ eV and $E_2=5$ eV. The use of the CCC calculated amplitudes or the 4P parametrization with the set of parameters extracted from the CCC calculation produce TDCS that are hardly discernible, thereby supporting this parametrization as a general scheme

TABLE II. Gaussian parameters of the He DPI at $E_1=35$ eV and $E_2=5$ eV.

Width (deg)		Magnitude			Phase shift, degree
Γ_g	Γ_u	b_g	gb_u	b_u/b_u	$\delta_g-\delta_u$
CCC calculation					
96 ± 2	69 ± 2	6.4 ± 0.2	1.6 ± 0.2	0.25 ± 0.04	122 ± 2 (-238 ± 2)
Cvejanović and Reddish [20]					
3P	98 ± 1			0.25 ± 0.01	$\pm246\pm2$
Bolognesi *et al.* [7]					
3P	102 ± 1			0.25 ± 0.01	$\pm232\pm2$
4P	104 ± 1	76 ± 2		0.25 ± 0.01	$\pm229\pm2$

over a broad kinematical range. However, the presently calculated Gaussian parameters are quite different from those obtained by fitting the experimental TDCS. This reflects on the uncertainty of the fit obtained from limited statistical accuracy of the experimental data, and also on the stability of the TDCS with respect to the parameters.

Clear deviations from the Gaussian ansatz are visible at small mutual angles where the antisymmetric amplitude acquires significant ''wings'' and its phase shows strong irregularities. These deviations do not show up in the TDCS as they fall into the mutual angle region where both amplitudes are small. Nevertheless, it would be interesting to investigate further if these deviations reflect different physics of the two-electron escape in parallel directions.

With the emergence of computationally intensive theories that aim to fully solve atomic ionization problems, such as the ECS method of Rescigno *et al.* [4], TDCC method of Colgan, Pindzola, and Robicheaux [2], HRM-SOW method of Malegat, Selles and Kazansky [3], and the CCC method, comparison can be made using a complete set of ionization amplitudes such as those presented in Fig. 1. This is further supported by emergence of experimental techniques whose goal is to perform a complete experiment and thereby fully test the calculated amplitudes [9].

ACKNOWLEDGMENTS

The authors wish to thank S. Cvejanović for many fruitful discussions. The Australian Partnership for Advanced Computing is acknowledged for providing access to the Compaq AlphaServer SC National Facility.

[1] J. S. Briggs and V. Schmidt, J. Phys. B **33**, R1 (2000).
[2] J. Colgan, M. S. Pindzola, and F. Robicheaux, J. Phys. B **34**, L457 (2001).
[3] L. Malegat, P. Selles, and A. K. Kazansky, Phys. Rev. Lett. **85**, 4450 (2000).
[4] T. N. Rescigno, M. Baertschy, W. A. Isaacs, and C. W. McCurdy, Science **286**, 2474 (1999).
[5] M. Baertschy, T. N. Rescigno, and C. W. McCurdy, Phys. Rev. A **64**, 022709 (2001).
[6] S. Cvejanović, J. P. Wightman, T. Reddish, F. Maulbetsch, M. A. MacDonald, A. S. Kheifets, and I. Bray, J. Phys. B **33**, 265 (2000).
[7] P. Bolognesi, R. Camilloni, M. Coreno, G. Turri, J. Berakdar, A. Kheifets, and L. Avaldi, J. Phys. B **34**, 3193 (2001).
[8] C. Dawson, S. Cvejanovic̀, D. P. Seccombe, T. J. Reddish, F. Maulbetsch, A. Huetz, J. Mazeau, and A. S. Kheifets, J. Phys. B **34**, L525 (2001).
[9] B. Kraessig, in The International Symposium on $(e,2e)$, Double Photoionization and Related Topics, Rolla, MO (unpublished).
[10] A. Huetz, P. Selles, D. Waymel, and J. Mazeau, J. Phys. B **24**, 1917 (1991).
[11] L. Malegat, P. Selles, and A. Huetz, J. Phys. B **30**, 251 (1997).
[12] L. Malegat, P. Selles, P. Lablanquie, J. Mazeau, and A. Huetz, J. Phys. B **30**, 263 (1997).
[13] A. R. P. Rau, J. Phys. B **9**, L283 (1976).
[14] J. M. Feagin, J. Phys. B **17**, 2433 (1984).
[15] A. K. Kazansky and V. N. Ostrovsky, Phys. Rev. A **48**, R871 (1993).
[16] O. Schwarzkopf and V. Schmidt, J. Phys. B **28**, 2847 (1995).
[17] J. P. Wightman, S. Cvejanović, and T. J. Reddish, J. Phys. B **31**, 1753 (1998).
[18] S. Cvejanović (unpublished).
[19] A. S. Kheifets and I. Bray, Phys. Rev. A **62**, 065402 (2000).
[20] S. Cvejanović and T. Reddish, J. Phys. B **33**, 4691 (2000).
[21] F. Maulbetsch and J. S. Briggs, J. Phys. B **27**, 4095 (1994).
[22] A. S. Kheifets and I. Bray, J. Phys. B **31**, L447 (1998).
[23] A. Huetz, L. Andric, A. Jean, P. Lablanquie, P. Selles, and J. Mazeau, in *The Physics of Electronic and Atomic Collisions*, edited by L. J. Dubé, J. B. A. Mitchel, J. W. McConkey, and C. Brion, AIP Conf. Proc. No. 360 (AIP, Woodbury, NY, 1995), pp. 139–151.
[24] K. Soejima, A. Danjo, K. Okuno, and A. Yagishita, Phys. Rev. Lett. **83**, 1546 (1999).
[25] S. J. Schaphorst, B. Krassing, O. Schwarzkopf, N. Scherer, V. Schmidt, P. Lablanquie, L. Andric, J. Mazeau, and A. Huetz, J. Electron Spectrosc. Relat. Phenom. **76**, 229 (1995).
[26] A. S. Kheifets and I. Bray, Phys. Rev. Lett. **81**, 4588 (1998).
[27] D. A. Varshalovich, A. N. Moskalev, and V. K. Khersonskii, *Quantum Theory of Angular Momentum* (World Scientific, Singapore, 1988).
[28] A. Kono and S. Hattori, Phys. Rev. A **29**, 2981 (1984).
[29] M. Abramowitz and I. A. Stegun, *Handbook of Mathematical Functions with Formulas, Graphs, and Mathematical Tables* (Academic, New York, 1975).
[30] I. Bray, Phys. Rev. Lett. **78**, 4721 (1997).
[31] A. T. Stelbovics, Phys. Rev. Lett. **83**, 1570 (1999).
[32] I. Bray, J. Phys. B **33**, 581 (2000).
[33] O. Schwarzkopf, B. Krassig, J. Elmiger, and V. Schmidt, Phys. Rev. Lett. **70**, 3008 (1993).
[34] R. Dörner *et al.*, Phys. Rev. A **57**, 1074 (1998).
[35] H. Bräuning *et al.*, J. Phys. B **31**, 5149 (1998).
[36] V. Mergel *et al.*, Phys. Rev. Lett. **80**, 5301 (1998).